Article

A 10-Å Spectroscopic Ruler Applied to Short Polyprolines

Harekrushna Sahoo, Danilo Roccatano, Andreas Hennig, and Werner M. Nau

J. Am. Chem. Soc., **2007**, 129 (31), 9762-9772• DOI: 10.1021/ja072178s • Publication Date (Web): 13 July 2007

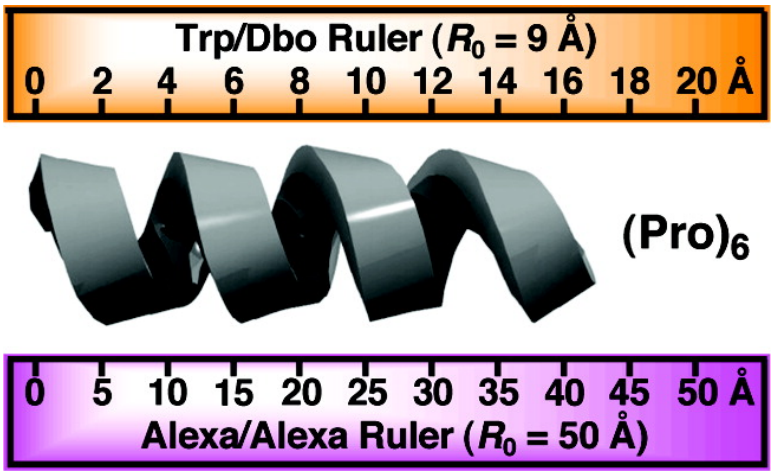

J|A|C|S
ARTICLES
Published on Web 07/13/2007

A 10-Å Spectroscopic Ruler Applied to Short Polyprolines

Harekrushna Sahoo, Danilo Roccatano, Andreas Hennig, and Werner M. Nau*

Contribution from the School of Engineering and Science, Jacobs University Bremen, Campus Ring 1, D-28759 Bremen, Germany

Received March 28, 2007; E-mail: w.nau@jacobs-university.de

Abstract: Fluorescence resonance energy transfer (FRET) from the amino acid tryptophan (Trp) as donor and a 2,3-diazabicyclo[2.2.2]oct-2-ene-labeled asparagine (Dbo) as acceptor in peptides of the general structure Trp-$(Pro)_n$-Dbo-NH_2 ($n = 1-6$) was investigated by steady-state and time-resolved fluorescence, CD, and NMR spectroscopy as well as by molecular dynamics (MD) simulations (GROMOS96 force field). The Trp/Dbo FRET pair is characterized by a very short Förster radius (R_0 ca. 9 Å), which allowed distance determinations in such short peptides. Water and propylene glycol were investigated as solvents. The peptides were designed to show an early nucleation of the poly(Pro)II (PPII) secondary helix structure for $n \geq 2$, which was confirmed by their CD spectra. The shortest peptide ($n = 1$) adopts preferentially the *trans* conformation about the Trp-Pro bond, as confirmed by NMR spectra. The FRET efficiencies ranged 2−72% and were found to depend sensitively on the peptide length, i.e., the number of intervening proline residues. The analysis of the FRET data at different levels of theory (assuming either a fixed distance or distance distributions according to a wormlike chain or Gaussian model) afforded donor−acceptor distances between ca. 8 Å ($n = 1$) and ca. 16 Å ($n = 6$) in water, which were found to be similar or slightly higher in propylene glycol. The distances afforded by the Trp/Dbo FRET pair were found to be reasonable in comparison to literature data, expectations from the PPII helix structure, and the results from MD simulations. The persistence lengths for the longer peptides were found to lie at 30−70 Å in water and 220 ± 40 Å in propylene glycol, suggesting a more rigid PPII helical structure in propylene glycol. A detailed comparison with literature data on FRET in polyprolines demonstrates that the donor−acceptor distances extracted by FRET are correlated with the Förster radii of the employed FRET pairs. This demonstrates the limitations of using FRET as a spectroscopic ruler for short polyprolines, which is presumably due to the breakdown of the point dipole approximation in Förster theory, when the size of the chromophores becomes comparable or larger than the distances under investigation.

Introduction

Förster theory predicts that the rate of fluorescence resonance energy transfer (FRET) should fall off steeply (R^{-6}) with increasing distance between donor (D) and acceptor (A).[1] The FRET efficiency (E) depends on the Förster radius (R_0) of the D/A pair, which determines at which distance 50% energy transfer occurs. Stryer and Haugland (S&H) 40 years ago reported FRET experiments with dansyl (Dns) as the amino-terminal acceptor and naphthyl (Naph) as the carboxy-terminal donor spaced by 1−12 proline residues,[2] which had then been recognized to form a rigid biomolecular backbone in aqueous solution: the poly(Pro)II (PPII) helix.[3] The authors found that the predicted R^{-6} distance dependence was nicely reproduced by the experimental results. This seminal study has subsequently been considered as a "proof" of Förster theory and, arguably, has contributed a major share to the recognition of FRET as a powerful tool for distance determinations, in particular in the biosciences.[4−8]

The advent of single-molecule fluorescence detection techniques has led to a renaissance of FRET,[9−15] and this technique has very recently been applied by several authors to polyprolines,[15−17] thereby testing once more the usefulness of FRET as a "spectroscopic ruler". With these recent studies, additional independent experimental FRET efficiencies of polyprolines have become available, in particular for longer polyprolines ($n \geq 6$), from which the D−A distances as well as distribution

(1) Förster, T. *Ann. Phys.* **1948**, *437*, 55−75.
(2) Stryer, L.; Haugland, R. P. *Proc. Natl. Acad. Sci. U.S.A.* **1967**, *58*, 719−726.
(3) Cowan, P. M.; McGavin, S. *Nature* **1955**, *176*, 501−503.
(4) Stryer, L. *Ann. Rev. Biochem.* **1978**, *47*, 819−846.
(5) Fairclough, R. H.; Cantor, C. R. *Methods Enzymol.* **1978**, *48*, 347−379.
(6) Wu, P.; Brand, L. *Anal. Biochem.* **1994**, *218*, 1−13.
(7) Selvin, P. R. *Methods Enzymol.* **1995**, *246*, 300−334.
(8) Lakowicz, J. R. *Principles of fluorescence spectroscopy*, 2nd ed.; Kluwer Academic/Plenum: New York, 1999.
(9) Deniz, A. A.; Dahan, M.; Grunwell, J. R.; Ha, T.; Faulhaber, A. E.; Chemla, D. S.; Weiss, S.; Schultz, P. G. *Proc. Natl. Acad. Sci. U.S.A.* **1999**, *96*, 3670−3675.
(10) Deniz, A. A.; Laurence, T. A.; Beligere, G. S.; Dahan, M.; Martin, A. B.; Chemla, D. S.; Dawson, P. E.; Schultz, P. G.; Weiss, S. *Proc. Natl. Acad. Sci. U.S.A.* **2000**, *97*, 5179−5184.
(11) Weiss, S. *Nat. Struct. Biol.* **2000**, *7*, 724−729.
(12) Selvin, P. R. *Nat. Struct. Biol.* **2000**, *7*, 730−734.
(13) Ha, T. *Curr. Opin. Struct. Biol.* **2001**, *11*, 287−292.
(14) Haas, E. *ChemPhysChem* **2005**, *6*, 858−870.
(15) Schuler, B.; Lipman, E. A.; Steinbach, P. J.; Kumke, M.; Eaton, W. A. *Proc. Natl. Acad. Sci. U.S.A.* **2005**, *102*, 2754−2759.
(16) Rüttinger, S.; Macdonald, R.; Krämer, B.; Koberling, F.; Roos, M.; Hildt, E. *J. Biomed. Optics* **2006**, *11*, 024012/1−02401279.
(17) Watkins, L. P.; Chang, H.; Yang, H. *J. Phys. Chem. A* **2006**, *110*, 5191−5203.

10.1021/ja072178s CCC: $37.00

Table 1. Reported Energy Transfer Efficiencies (*E*) and Effective Donor−Acceptor Distances (R_{eff}) (from eq 1) Determined from Different FRET Pairs in Dependence on the Number of Prolines (*n*) Separating Donor and Acceptor (see Supporting Information for an Expanded Table)

n	*E*	R_{eff}/Å	R_0/Å	FRET pair	solvent	method[a]	ref
1	1.00	−	27.2	Naph/Dns	ethanol	ss	2
	0.72	7.9	9.0	Trp/Dbo	H_2O	ss + tr	this work
	0.55	8.8	8.7	Trp/Dbo	PG[b]	ss + tr	this work
2	0.95[c]	16.5	27.2	Naph/Dns	ethanol	ss	2
	0.67	8.3	9.0	Trp/Dbo	H_2O	ss + tr	this work
	0.26	10.4	8.7	Trp/Dbo	PG[b]	ss + tr	this work
3	0.98[c]	14.2	27.2	Naph/Dns	ethanol	ss	2
4	0.97	14.9	27.2	Naph/Dns	ethanol	ss	2
	0.15	12.4	9.0	Trp/Dbo	H_2O	ss + tr	this work
	0.083	13.1	8.7	Trp/Dbo	PG[b]	ss + tr	this work
5	0.80[c]	20.4	27.2	Naph/Dns	ethanol	ss	2
6	0.78[c]	22.0	27.2	Naph/Dns	ethanol	ss	2
	0.74	20.3	24.2	Trp/Dns	PG[b]	tr	19
	0.95	33.1	54	Alexa 488/594	H_2O	smd	15
	0.90	37.4	54	Alexa 488/594	H_2O	tr	15
	0.79	40.9	51	Alexa 555/647	H_2O	smd/pie	16
	0.90	35.4	51	Alexa 555/647	H_2O	smd[d]	16
	0.041	16.6	9.0	Trp/Dbo	H_2O	ss + tr	this work
	0.024	16.5	8.7	Trp/Dbo	PG[b]	ss + tr	this work
12	0.16	35.9	27.2	Naph/Dns	ethanol	ss	2
	0.83	38.1	51	Alexa 555/647	H_2O	smd	17
	0.84	40.9	54	Alexa 488/594	H_2O	smd	15
	0.67	45.3	51	Alexa 555/647	H_2O	smd/pie	16
	0.83	39.2	51	Alexa 555/647	H_2O	smd[d]	16

[a] Abbreviations used: ss, steady-state; tr, time-resolved; smd, single-molecule fluorescence detection; pie, pulsed interleaved excitation. [b] Propylene glycol. [c] The efficiencies for $n = 2-11$ were read from Figure 4 in ref 2. [d] Uncorrected (apparent) values.

functions were derived. For the sake of quick inspection and comparison, we report in Table 1 the mean FRET efficiencies and effective D−A separations (R_{eff}) obtained by the simple Förster formula in eq 1:

$$R_{eff} = \sqrt[6]{R_0^6 \frac{1-E}{E}} \qquad (1)$$

When comparing experiment and theory, Schuler et al.[15] showed that the distances determined by FRET and Förster theory for the longer polyprolines ($n \gg 12$) were much smaller than anticipated from a rigid PPII helix. These marked deviations were assigned to a higher than previously presumed flexibility of *long* polyprolines. S&H had also applied FRET as a spectroscopic ruler to *short* polyprolines ($n < 8$), but the performance in this short-distance range was not systematically tested thereafter. The purpose of the present study is therefore to reinvestigate D−A distances in such short polyprolines by FRET. Toward this end, we utilize our recently communicated short-distance Trp/Dbo FRET pair (Scheme 1),[18] which has proven advantageous in the determination of short distances in the 10-Å range. The near-UV absorption of the parent acceptor chromophore (DBO, Scheme 1) is characterized by a very low oscillator strength, which results in an exceedingly small spectral overlap and consequently R_0 value of about 9 Å in peptides, a factor of 3−6 smaller than those of previously employed FRET pairs.[2,15−17,19] Moreover, and in contrast to the study by S&H, we designed peptide sequences with an early onset of PPII helix

Scheme 1 . Molecular Structures of the Investigated Chromophore, Labeled Amino Acid, and Peptides

2,3-diazabicyclo[2.2.2]oct-2-ene
DBO

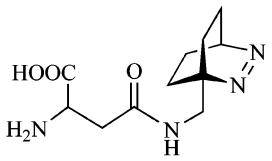

DBO-labeled asparagine
(Dbo)

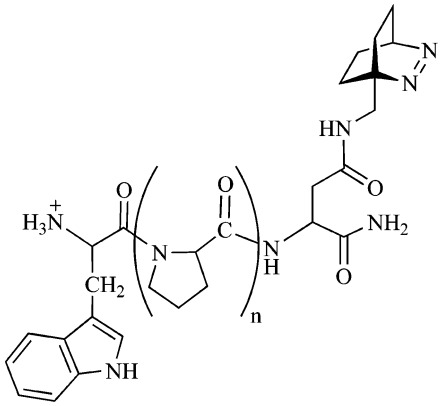

Trp-(Pro)$_n$-Dbo-NH$_2$

structure formation ($n \geq 2$) in order to facilitate comparison with longer polyprolines.

Results

Trp-(Pro)$_n$-Dbo-NH$_2$ peptides ($n = 1$, 2, 4, and 6, Scheme 1) containing the amino acid Trp as the amino-terminal donor and Dbo as the carboxy-terminal acceptor were prepared by solid-phase synthesis. For reference purposes, we also investigated one donor-only labeled peptide Trp-(Pro)$_6$-NH$_2$, one acceptor-only labeled peptide, (Pro)$_4$-Dbo-NH$_2$, and the parent chromophores (Trp and DBO).

Calculation of Förster Radii. The R_0 values were calculated from the spectral overlap (*J*) between the corrected fluorescence and UV absorption spectra of the reference peptides (Figure 1).[18] The local refractive index of the peptide-bound chromophores was taken as 1.340 in water[18] and 1.432 in propylene glycol.[20] The orientation factor (κ^2) was assumed to be $^2/_3$; *cf.* Supporting Information. The donor fluorescence quantum yield of the Trp-(Pro)$_6$-NH$_2$ peptide was experimentally determined with reference to that of free Trp ($\Phi_D = 0.13$ in water).[8] Expectedly, the Trp residue in peptides shows a significantly reduced fluorescence quantum yield compared to the free amino acid.[19,21] The resulting R_0 values for different combinations are compiled in Table 2. Herein, we used values of 9.0 and 8.7 Å

(18) Sahoo, H.; Roccatano, D.; Zacharias, M.; Nau, W. M. *J. Am. Chem. Soc.* **2006**, *128*, 8118−8119.
(19) Lakowicz, J. R.; Wiczk, W.; Gryczynski, I.; Johnson, M. L. *Proc. SPIE* **1990**, *1204*, 192−205.
(20) Lide, D. R. *Handbook of chemistry and physics*, 84th ed.; CRC Press: Boca Raton, FL, 2003.
(21) Chen, R. F.; Knutson, J. R.; Ziffer, H.; Porter, D. *Biochemistry* **1991**, *30*, 5184−5195.

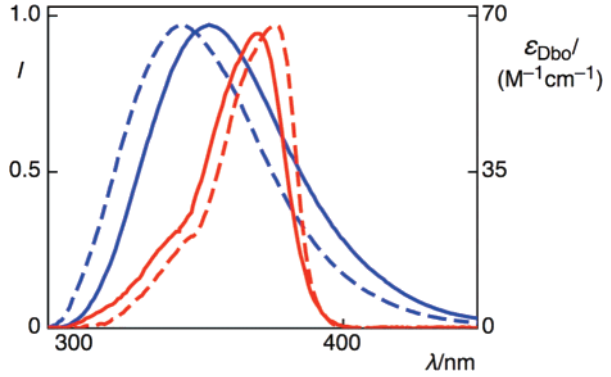

Figure 1. Spectral overlap of the Trp emission (blue) and Dbo absorption spectrum (red) in water (solid line) and propylene glycol (dashed), obtained for the respective single-labeled reference peptides; for the fluorescence spectrum of the acceptor see Figure S-2 in the Supporting Information.

Table 2. Photophysical Parameters and Förster Radii for the Trp/Dbo FRET Pair in Its Free Form and the Respective Donor-Only and Acceptor-Only Labeled Polyprolines in Water and Propylene Glycol (PG)

donor/acceptor	solvent	$J/(10^{11}\,M^{-1}\,cm^{-1}\,nm^4)$	Φ_D[a]	R_0/Å
Trp/DBO	H_2O	4.15	0.13[b]	10.0
	PG	4.45	0.22	10.2
Trp-$(Pro)_6$-NH_2/DBO	H_2O	4.16	0.057	8.8
	PG	4.09	0.11	9.3
Trp/$(Pro)_4$-Dbo-NH_2	H_2O	5.07	0.13[b]	10.3
	PG	4.41	0.22	10.2
Trp-$(Pro)_6$-NH_2/$(Pro)_4$-Dbo-NH_2	H_2O	5.09	0.057	**9.0**
	PG	4.01	0.11	**8.7**

[a] 5% error. [b] Reference value, from ref 8.

in water and propylene glycol, respectively. The very small R_0 value is a special characteristics of the Trp/Dbo FRET pair, which makes distance determinations in short peptides feasible.[18,22] Note that the absence of Dbo absorbance at 280 nm (Figure 1) ensures a perfectly selective laser excitation of the donor Trp, which greatly facilitates the experimental design and quantitative analysis of the FRET data.

Donor Fluorescence. Steady-state fluorescence spectra (λ_{exc} = 280 nm, Figure 2) as well as excitation spectra (λ_{obs} = 350 nm) were recorded in water and propylene glycol. The fluorescence intensities of the donor Trp in the different peptides (Table 3) were directly determined from the intensities at the fluorescence maximum (355 ± 2 nm in water, 350 ± 2 nm in propylene glycol) relative to that of the donor-only substituted reference. Because the acceptor neither fluoresces below 370 nm nor absorbs at the excitation wavelength (Figure 1), no additional corrections were required.

The time-resolved fluorescence decays of Trp (by time-correlated single photon counting, λ_{exc} = 280 nm, λ_{obs} = 350 nm, Figure 3) were also measured in both solvents; the decays were generally non-monoexponential, but a biexponential decay function allowed for satisfactory fitting in all cases ($\chi^2 < 1.1$); the resulting average fluorescence lifetimes are entered in Table 3. The relative donor fluorescence intensities (I_{DA}) and lifetimes (τ_{DA}) in the D/A-substituted peptides were expectedly smaller than those of the donor-only substituted reference peptide (I_D, τ_D). The steady-state and time-resolved FRET efficiencies (Table 4) were calculated as $E_{ss} = 1 - I_{DA}/I_D$ and $E_{tr} = 1 - \tau_{DA}/\tau_D$,

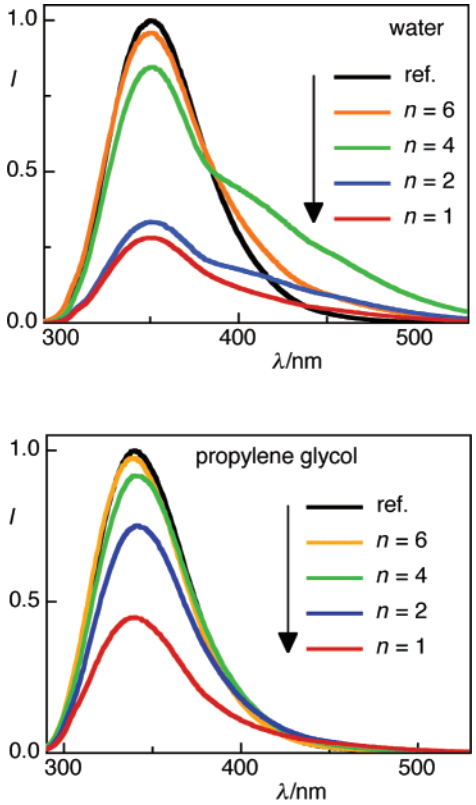

Figure 2. Steady-state fluorescence spectra of the Trp-$(Pro)_n$-Dbo-NH_2 peptides in water (top) and propylene glycol (bottom) relative to the fluorescence decay of the Trp-$(Pro)_6$-NH_2 reference peptide lacking the acceptor (black spectrum).

Table 3. Relative Donor Fluorescence Intensities and Lifetimes in Trp-$(Pro)_n$-Dbo-NH_2 Peptides in Water and Propylene Glycol (PG)

	I^a		τ^b/ns	
n	water	PG	water	PG
reference[c]	1.000	1.000	1.94[d]	2.15[e]
1	0.28	0.45	0.70	1.30
2	0.36	0.74	0.76	1.62
4	0.87	0.917	1.74	1.98
6	0.974	0.976	1.89	2.10

[a] Relative donor fluorescence intensities, determined from two independent emission and one excitation spectral measurement (λ_{obs} = 350 nm); error ±0.02 for n = 1−4 and ±0.010 for n = 6. [b] Average fluorescence lifetimes calculated as $\tau_{avg} = \alpha_1\tau_1 + \alpha_2\tau_2$ from two independent measurements; 3% statistical error (σ) obtained from fitting. [c] Reference peptide: Trp-$(Pro)_6$-NH_2. [d] Lifetime components from biexponential fitting were τ_1 = 1.53 ns (α_1 = 0.60) and τ_2 = 2.57 (α_2 = 0.40). [e] Lifetime components from biexponential fitting were τ_1 = 1.37 ns (α_1 = 0.75) and τ_2 = 4.53 ns (α_2 = 0.25).

respectively. The FRET efficiency was quite large for the shortest peptides (up to 72%), decreased steeply with length, and became as small as 2% for the hexaproline peptide. Longer polyprolines were consequently not examined, because FRET would have become experimentally insignificant. As can be seen, the Trp/Dbo FRET pair is ideally suited for investigating short polyprolines, with highly significant variations in FRET efficiency between n = 1−6.

The steady-state FRET efficiencies were directly employed to calculate effective D−A separations with the simple Förster formula (eq 1). Equation 1 holds strictly only for fixed D−A distances but is generally well suited to assess approximate distances and relative trends. In fact, for the rigid proline peptides studied herein, a refined analysis of FRET data by

(22) Sahoo, H.; Nau, W. M. *ChemBioChem* **2007**, *8*, 567−573.

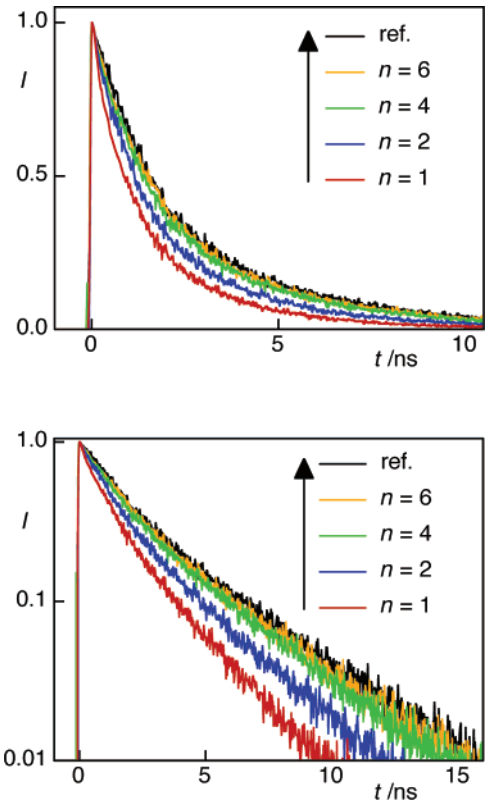

Figure 3. Time-resolved fluorescence decays of Trp-(Pro)$_n$-Dbo-NH$_2$ peptides in propylene glycol (normalized, linear intensity scale on the top and logarithmic one on the bottom) relative to the fluorescence decay of the Trp-(Pro)$_6$-NH$_2$ reference peptide lacking the acceptor (black trace).

Table 4. Steady-State and Time-Resolved FRET Efficiencies in Trp-(Pro)$_n$-Dbo-NH$_2$ Peptides and Static Quenching Component in Water and Propylene Glycol (PG)

	E_{ss}[a,b]		E_{tr}[b,c]		F[d]	
n	water	PG	water	PG	water	PG
1	0.72	0.55	0.64	0.39	0.08	0.16
2	0.64	0.26	0.61	0.25	0.03	0.01
4	0.13	0.083	0.10	0.079	0.03	0.004
6	0.026	0.024	0.026	0.023	0.000	0.001

[a] Steady-state energy transfer efficiencies. [b] Error ±0.02 for n = 1−4 and ±0.010 for n = 6. [c] Energy transfer efficiency obtained from time-resolved fluorescence (average donor lifetimes). [d] Fraction of static quenching, calculated as $F = E_{ss} - E_{tr}$; error ±0.03.

distribution models (see below) does not lead to major changes. As exemplified previously,[18,22] the FRET efficiencies from the time-resolved experiments need to be "corrected" for a static quenching component (F in Table 4), which takes into account a small fraction of conformations, which are in contact (assumed van der Waals distance 4.0 Å) when excitation occurs, and which escape from the time-resolved detection due to immediate quenching by FRET.[23] This correction was performed by using eq 2, and the resulting effective D−A distances from the time-resolved measurements were in good agreement with those from the steady-state data (Table S-1 of Supporting Information). Table 5 provides the effective D−A distances as averages of both sets of experiments. As can be seen, the R_{eff} values in

(23) The static quenching fraction was significant (>3%) only for the shortest peptide (n = 1, Table 4) and therefore not analyzed in detail. A small population of conformations with donor−acceptor contact appears reasonable for the shortest peptide, because the attachment of donor and acceptor allows for some flexibility.

Table 5. Effective Donor−Acceptor Distances (R_{eff}), Persistence Lengths (l_p), and Contour Lengths (l_c) Determined from FRET in Trp-(Pro)$_n$-Dbo-NH$_2$ Peptides As Analyzed by a Wormlike-Chain Model in Water and Propylene Glycol (PG)

	R_{eff}[a]/Å		l_p[b,c]/Å		l_c[b,d]/Å	
n	water	PG	water	PG	water	PG
1	7.8	8.4	130	290	8.3	9.4
2	8.2	10.3	66	250	8.5	10.6
4	12.3	13.1	45	210	13.2	13.2
6	16.6	16.5	30	180	15.7	16.3

[a] Average of the effective donor−acceptor distances determined from steady-state and time-resolved FRET efficiencies according to eqs 1 and 2; *cf.* Table S-1 in Supporting Information for error limits. [b] Calculated by using eq 3 in combination with a wormlike-chain distribution function. [c] 25% error. [d] 5% error.

propylene glycol increased systematically from ca. 8.4 Å for n = 1 to ca. 16.5 Å for n = 6. A similar trend applied in water, although the increase upon going from n = 1 to 2 was quite small in this case. Note that the variations in effective D−A distances of the polyprolines in water and the 45 times[20] more viscous propylene glycol were rather small (Table 5), except for n = 2 (2.1 Å longer).

$$R_{eff} = (1 - F)\left\{R_0^6\left(\frac{1}{E_{tr}} - 1\right)\right\}^{1/6} + FR_{vdW} \qquad (2)$$

Distribution Function Analysis. Because diffusion-enhanced FRET is considered to be negligible in propylene glycol[18] and for the longer ($n \geq 2$) polyprolines (see Supporting Information), the time-resolved fluorescence decays could be further employed to extract more detailed information regarding the distribution function of D−A distances, $P(R)$.[19,24] Accordingly, the decays were fitted according to eq 3, where α_i and $\tau_{D,i}$ were taken as the preexponential factors and lifetimes of the decay components in the absence of the acceptor.[18,22]

$$I_{DA}(t) = I_0 \int P(R) \sum_i \alpha_i \exp\left[-\frac{t}{\tau_{D,i}}\left(1 + \left(\frac{R_0}{R}\right)^6\right)\right] dR$$

where

$$P(R) = \frac{4\pi NR^2}{l_c^2[1 - (R/l_c)^2]^{9/2}} \exp\left(-\frac{3l_c}{4l_p[1 - (R/l_c)^2]}\right) \qquad (3)$$

(for wormlike chain model)

$$\text{or } P(R) = \frac{1}{\sigma\sqrt{2\pi}} \exp\left[-\frac{1}{2}\left(\frac{R - R_{mean}}{\sigma}\right)\right]$$

(for Gaussian model)

The corresponding analysis further requires a probability distribution to be chosen, which was implemented within a numerical integration procedure for fitting.[25] We employed both a function derived from a wormlike chain model (N is a normalization factor)[26] and a Gaussian distribution function (eq 3).[8] The use of the wormlike chain function affords as fitting

(24) Cantor, C. R.; Pechukas, P. *Proc. Natl. Acad. Sci. U.S.A.* **1971**, *68*, 2099−2101.
(25) ProFit 6.0.3 ed., 2005; QuantumSoft: Zürich, Switzerland.
(26) Thirumalai, D.; Ha, B.-Y. Statistical Mechanics of Semiflexible Chains: A meanfield variational approach. In *Theoretical and Mathematical Models in Polymer Research*; Grossberg, A., Ed.; Academia: New York, 1998; pp 1−35.

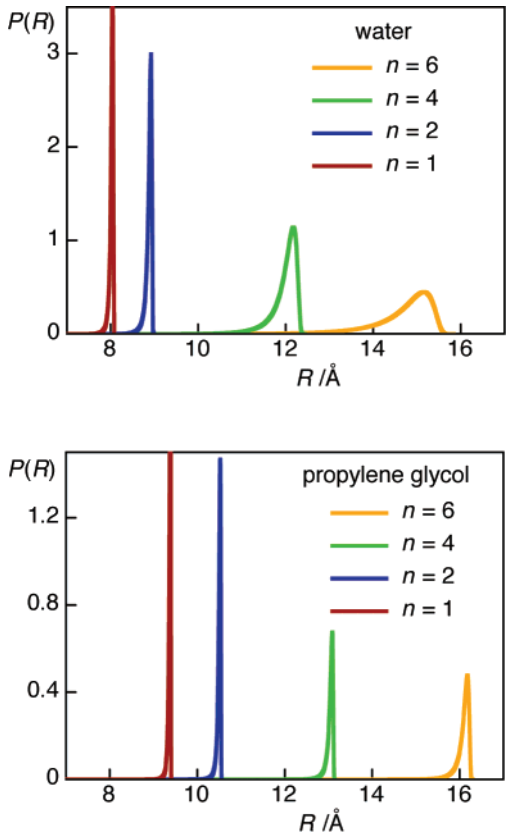

Figure 4. Distribution functions recovered from the analysis of the time-resolved fluorescence decays in H_2O (top) and propylene glycol (bottom) according to a wormlike chain distribution-dependent FRET kinetics. Note that the sharpest spike for $n = 1$ is cut off for clarity.

parameters the contour length l_c and the persistence length l_p; the Gaussian model yields the mean distance (R_{mean}) and standard deviation (σ) or half-width ($hw = 2.354\ \sigma$) of the function as comparable measures of the length and rigidity (broadness of distribution) of the peptide chain, respectively.[27]

The fits were very good ($\chi^2 < 1.1$) for both distribution functions. The recovered distributions and parameters for the wormlike chain model are shown in Figure 4 and Table 5, while those for the Gaussian model are contained in the Supporting Information (Figure S-1 and Table S-2). Note that the persistence lengths (or half-widths) showed a large error and that the contour lengths (or mean distances) were very similar to the effective D−A distances extracted from eqs 1 and 2, as expected for *narrow distributions*.

Secondary Structure and *Trans*−*Cis* Isomers. The electronic circular dichroism (CD) spectra of the Trp-$(Pro)_n$-Dbo-NH_2 peptides in both water and propylene glycol (Figure 5) revealed the characteristic features for the PPII helical structure, namely the trough at 203 ± 1 nm, which becomes more pronounced as the number of proline peptide bonds increases.[28−30] Such CD spectra are diagnostic for a preferential *trans* conformation of the Trp-Pro peptide bond for $n = 1$[29] and a virtually quantitative population of the *trans* Pro−Pro bonds for $n \geq 2$.[28,29] The Dbo residue contributes little to the CD effect near 203 nm, because the spectra of Trp-$(Pro)_6$-Dbo-NH_2 and Trp-$(Pro)_6$-NH_2 are very similar. Peptides with PPII structure show frequently a positive band near 225 nm, whose relative intensity varies quite strongly with peptide structure (ca. 10−60 times weaker than the trough)[28,31] and vanishes in some cases.[32−34] This secondary feature was almost absent ($\lambda_{max} =$ 227 nm, ca. 100 times weaker than the trough) in the reference peptide, $(Pro)_4$-Dbo-NH_2, which may be due to the Dbo-NH_2 terminus. The sizable positive CD band near 224 ± 1 nm observed for the Trp-$(Pro)_n$-Dbo-NH_2 peptides is therefore assigned to contributions from Trp.

Spectral similarities become most apparent when the ellipticity is normalized to the number of proline peptide bonds (θ', Figure 5, bottom).[35] The "proline residue" molar ellipticity obtained in this way for the trough (ca. 46×10^4 deg cm^2 dmol^{-1}) lies in the upper range of CD intensities reported for polyprolines.[29,31] For comparison purposes, we also recorded the CD spectra of the dipeptide Trp-Pro-OH (at pH 2, dominant *trans* form) and Trp-Pro-O^- (at pH 7, dominant *cis* form).[29,36,37] Evidently, the CD features of the latter lack the trough near 203 nm and therefore stand in contrast, suggesting that all other spectra correspond to dominant *trans* peptide bonds. Most importantly, the depths of the troughs are the same, within error, for the Trp-$(Pro)_n$-Dbo-NH_2 peptides with $n \geq 2$ in both water and propylene glycol. This spectral feature provides strong support for the invariable structural assignment in these cases, namely the PPII helix. A slightly smaller intensity is observed for $n = 1$ and more pronounced for (*trans*) Trp-Pro-OH. This lower intensity is expected because the CD effects from the amino-terminal *cis* peptide bond (population ca. 30% in water and 25% in propylene glycol, see below) have their highest weight for the shortest peptides.

Comprehensive spectroscopic evidence for different model peptides demonstrates that the *hexa*proline backbone forms a stable PPII helix in aqueous solution.[2,28,29,38−44] For shorter

(27) In contrast to the Gaussian model (ref 19), wormlike distributions are somewhat more "realistic", especially in the case of flexible peptides, because they do not extend to distances larger than that of the most extended conformation, and because the distributions become negligibly small at distances below the van der Waals limit of ca. 4 Å. When applying the wormlike chain model, one can further calculate an average distance, which is somewhat shorter than the contour lengths due to the asymmetric shape of this distribution. The difference is less than 0.2 Å, except for $n = 4$ in water (0.6 Å smaller) and $n = 6$ in water (1.3 Å).

(28) Helbecque, N.; Loucheux-Lefebvre, M. H. *Int. J. Pept. Protein Res.* **1982**, *19*, 94−101.
(29) Wierzchowski, K. L.; Majcher, K.; Poznanski, J. *Acta Biochim. Pol.* **1995**, *42*, 259−268.
(30) Evidence for a significant population of the PPI helical structure, which is known to be favored for longer polyprolines (e.g., $n = 13$) in methanol and isopropanol (ref 31) was not obtained by CD. The shapes and intensities of the bands of the Trp-$(Pro)_n$-Dbo-NH_2 peptides in propylene glycol were very similar to those in (deuterated) water, even after the peptides had been incubated for several months (note that the PPII to PPI transition occurs within hours to days; *cf.* refs 31,32).
(31) Kakinoki, S.; Hirano, Y.; Oka, M. *Polym. Bull.* **2005**, *53*, 109−115.
(32) Dukor, R. K.; Keiderling, T. A. *Biospectroscopy* **1996**, *2*, 83−100.
(33) Schweitzer-Stenner, R.; Eker, F.; Perez, A.; Griebenow, K.; Cao, X.; Nafie, L. A. *Pept. Sci.* **2003**, *71*, 558−568.
(34) Whittington, S. J.; Chellgren, B. W.; Hermann, V. M.; Creamer, T. P. *Biochemistry* **2005**, *44*, 6269−6275.
(35) CD spectra are routinely reported as mean residue ellipticity, i.e., normalized for the total number of residues. In our case, the Dbo residue does not contribute significantly to the characteristic trough, as can be seen from the comparison of the CD spectra for Trp-$(Pro)_6$-NH_2 and Trp-$(Pro)_6$-Dbo-NH_2. It was consequently not counted as an amino acid contributing to this CD feature to allow a better absolute comparison.
(36) Grathwohl, C.; Wüthrich, K. *Biopolymers* **1976**, *15*, 2043−2057.
(37) Grathwohl, C.; Wüthrich, K. *Biopolymers* **1976**, *15*, 2025−2041.
(38) Vassilian, A.; Wishart, J. F.; van Hemelryck, B.; Schwarz, H.; Isied, S. S. *J. Am. Chem. Soc.* **1990**, *112*, 7278−7286.
(39) Bobrowski, K.; Holcman, J.; Poznański, J.; Ciurak, M.; Wierzchowski, K. L. *J. Phys. Chem.* **1992**, *96*, 10036−10043.
(40) Ogawa, M. Y.; Wishart, J. F.; Young, Z.; Miller, J. R.; Isied, S. S. *J. Phys. Chem.* **1993**, *97*, 11456−11463.
(41) Mishra, A. K.; Chandrasekar, R.; Faraggi, M.; Klapper, M. H. *J. Am. Chem. Soc.* **1994**, *116*, 1414−1422.
(42) Isied, S. S.; Ogawa, M. Y.; Wishart, J. F. *Chem. Rev.* **1992**, *92*, 381−394.

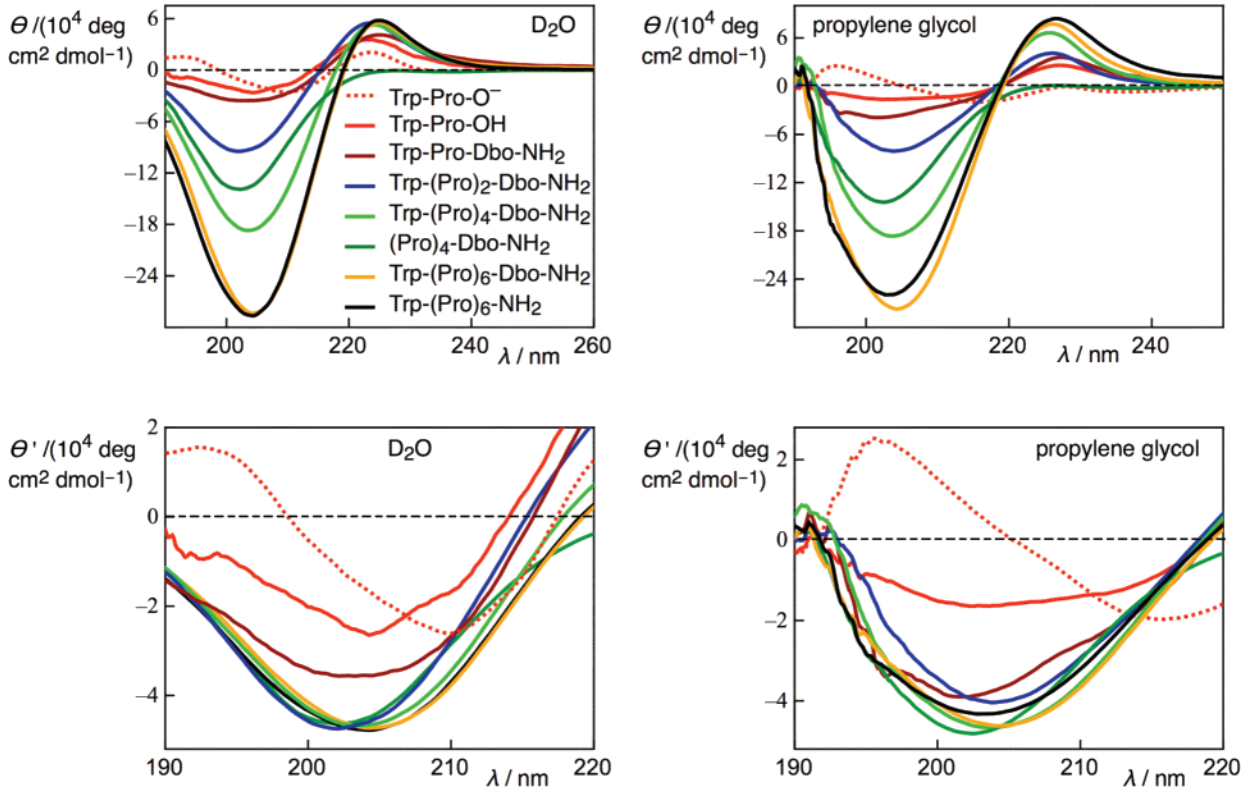

Figure 5. CD spectra of the Trp-(Pro)$_n$-Dbo-NH$_2$ and other model peptides in D_2O (left) and propylene glycol (right). The upper spectra show the molar ellipticity (per mole of peptide), and the bottom ones are normalized to the number of proline residues (per mole of proline peptide bond).

polyprolines, the onset of the PPII secondary structure may vary; for example, peptides of the type Gly-(Pro)$_n$-OH adopt the PPII structure only at $n = 3$ (onset),[28] those of the type (Pro)$_n$-OH[44] and Trp-(Pro)$_n$-Tyr-OH[29,45], only at $n = 4$, and the peptides used by S&H, only at $n = 5$.[2] The peptides investigated herein, however, were structurally optimized to adopt the characteristics of the PPII helical structure already at $n = 2$, similar to the situation for Trp-(Pro)$_n$-Met-OH peptides.[29] The early onset of secondary structure for such short peptides is less surprising if one considers recent spectroscopic evidence[33,46−49] which suggests that even single peptide bonds and non-proline containing tri- and tetrapeptides show characteristic features of the PPII structure.

The internal Pro−Pro bonds in the observed PPII helical structure adopt all-*trans* conformations.[3,50] In contrast, the *cis* isomers for rotation about the amino-terminal peptide bonds in polyprolines of the type Xaa-(Pro)$_n$ are known to be significantly populated as well.[51,52] We performed ^{1}H NMR measurements with the dipeptide Trp-Pro-Dbo-NH$_2$ (Figure S-3 in the Supporting Information) and found that the conformer with the *cis* orientation about the Trp-Pro bond was indeed significantly populated (ca. 30%), comparable to its abundance in Trp-Pro-OCH$_3$ (ca. 25%)[51] and peptides with internal Trp-Pro bonds (ca. 30−40%).[52,53] While the ^{1}H NMR spectrum of the shortest peptide ($n = 1$) could be comprehensively assigned, the spectra of the longer peptides were too complex to allow reliable assignments and quantifications of the *trans*−*cis* contributions. However, previous studies carried out for related peptides (Trp-(Pro)$_n$-Tyr) showed that the carboxyl extension of the polyproline backbone has no large effect on the amino-terminal *trans*/*cis* ratio.[29,38,51]

Knowledge of the conformational distribution, in the present case, also of the amino-terminal *trans*/*cis* ratios, is important for the interpretation of the fluorescence experiments, because isomerization about prolines is slow (minutes to hours for Xaa-Pro bonds,[52,54] and hours to days for internal Pro−Pro bonds[31,32,55]) in relation to the nanosecond time scale of fluorescence measurements. Consequently, fluorescence contributions from at least two distinct conformers need to be considered. In practice, we found that the fluorescence decays of the Trp-(Pro)$_6$-NH$_2$ reference peptide could be satisfactorily fitted with two fluorescence lifetime components. We attribute

(43) Malak, R. A.; Gao, Z.; Wishart, J. F.; Isied, S. S. *J. Am. Chem. Soc.* **2004**, *126*, 13888−13889.
(44) Okabayashi, H.; Isemura, T.; Sakakibara, S. *Biopolymers* **1968**, *6*, 323−330.
(45) It should be noted that the closely related Trp-(Pro)$_n$-Tyr-OH peptides, which show the onset for nucleation of the PPII helix only at $n = 4$, have been extensively employed in studies of long-range electron transfer in polyprolines (refs 39,41), which is also distance dependent and shows an interesting switch-over in mechanism for $n = 1−9$ (ref 43).
(46) Eker, F.; Griebenow, K.; Schweitzer-Stenner, R. *J. Am. Chem. Soc.* **2003**, *125*, 8178−8185.
(47) Gokce, I.; Woody, R. W.; Anderluh, G.; Lakey, J. H. *J. Am. Chem. Soc.* **2005**, *127*, 9700−9701.
(48) Chellgren, B. W.; Miller, A.-F.; Creamer, T. P. *J. Mol. Biol.* **2006**, *361*, 362−371.
(49) Schweitzer-Stenner, R.; Measay, T.; Kakalis, L.; Jordan, F.; Pizzanelli, S.; Forte, C.; Griebenow, K. *Biochemistry* **2007**, *46*, 1587−1596.
(50) Schimmel, P. R.; Flory, P. J. *Proc. Natl. Acad. Sci. U.S.A.* **1967**, *58*, 52−59.
(51) Poznański, J.; Ejchart, A.; Wierzchowski, K. L.; Ciurak, M. *Biopolymers* **1993**, *33*, 781−795.
(52) Reimer, U.; Scherer, G.; Drewello, M.; Kruber, S.; Schutkowski, M.; Fischer, G. *J. Mol. Biol.* **1998**, *279*, 449−460.
(53) The population of the *cis* isomer depends on the amino acid type and may vary in dependence on the type of carboxy-terminal amino acid (refs 37, 52), and the charge status (refs 36,51). The presence of carboxy-terminal aromatic amino acids, prominently Tyr, and a deprotonated carboxy terminus favor the relative population of the *cis* form for the same reasons that they tend to disrupt the PPII helix structure of short polyprolines; see above.
(54) Grathwohl, C.; Wüthrich, K. *Biopolymers* **1981**, *20*, 2623−2633.
(55) Bovey, F. A.; Hood, F. P. *Biopolymers* **1967**, *5*, 915−919.

the two components tentatively to the *trans* and *cis* forms, based on the presumed conformations of the indole ring, the expected quenching effects, and the observed magnitudes of the preexponential factors of the decay components (see Supporting Information). Unfortunately, our FRET analysis (see above) does not allow us to reliably recover multiple distributions as expected to arise from the two *trans*−*cis* isomers (or other involved rotamers). The pertinent FRET data were therefore simply interpreted according to eqs 1−3, i.e., as if the *trans* and *cis* form had the same D−A separation (or distribution). This assumption behind our data analysis is significant, but interestingly, the MD simulations (see below) revealed similar average D−A distances for the *trans* and *cis* conformers, such that the fitting of the experimental data with a single distribution provides apparently a reasonably averaged representation of the two forms.

MD Simulations. To get further insights into the structures and distances of the *trans* and *cis* forms for isomerization about the Trp-Pro bond, and to evaluate the relationship between the D−A distance (assessed by FRET) and the C_α—C_α distance, we performed short time-scale (50 ns) MD simulations with the GROMOS96 force field.[56] All Pro-Pro linkages were modeled in the *trans* form, consistent with the experimentally observed PPII helical structure and remained *trans* during the MD runs. Interestingly, the average D−A distances of the trans and cis Trp-Pro isomers do not differ by more than 0.8 Å (except for $n = 4$), which may rationalize that the FRET data can be fitted with a single distribution (see above).

In line with expectation, the MD-calculated average C_α—C_α distance was found to be shorter for the *cis* than that for the *trans* form. However, the average D−A distance was smaller for the *trans* than that for the *cis* form. Close inspection of the most populated structures (Figure 6) revealed that the Trp chromophore showed a tendency to fold back along the proline backbone, which is presumably a consequence of hydrophobic association. This resulted in a shortening of the D−A distance, which was pronounced for the *trans* form (Table 6). The modeled conformation of the Trp residue in the *cis* form was very similar to that predicted by NMR studies, i.e., with the adjacent Pro pyrrolidine ring positioned above the plane of the indole ring.[51,57]

Discussion

The investigation of the structural and dynamic properties of short polypeptides (up to ca. 20 residues) are of utmost importance for the understanding of the folding mechanism and function of proteins. Popular experimental techniques for the study of short polypeptides are NMR and CD spectroscopy. FRET has been less routinely applied, first because it generally occurs over distances larger (20−50 Å) than those characteristic for short polypeptides (5−20 Å) and second because of the challenges to deconvolute structural and dynamic information obtained in FRET experiments with such short peptides, which are generally random-coiled and consequently flexible.[19,58−60] Polyproline presents an exception in this respect, because its high propensity to form secondary structures already at short

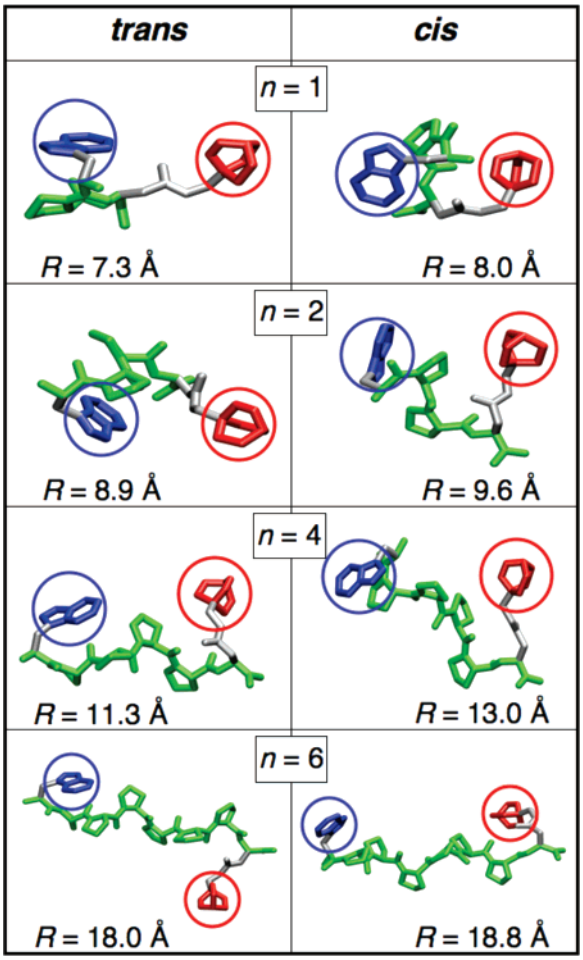

Figure 6. Representative structures from the most populated clusters obtained from the different simulations. Proline backbone is green, donor chromophore is blue, acceptor chromophore is red, and tethers/linkers are gray.

Table 6. Donor−Acceptor Distances Obtained from MD Simulations[a]

	R_{MD}(D–A)/Å		R_{MD}(C_α–C_α)/Å	
n	*trans*	*cis*	*trans*	*cis*
1	7.3	8.0	6.3	5.0
2	8.9	9.6	8.9	8.0
4	11.3	13.0	15.0	13.8
6	18.0	18.8	20.7	19.6

[a] Average distance between the centers of the indole ring and the azo group (*cf.* Figure 6) obtained from MD simulations (GROMOS96 force field) for 250 000 conformations sampled every 0.2 ps during a 50-ns MD run.

length and the cyclic proline residue itself allow relatively rigid and elongated backbones to be obtained. These spacers have proven highly attractive, on one hand to study their structures by substitution with *energy* donors and acceptors (FRET),[2,15−17,19] on the other hand to study functional aspects by substitution with *electron* donors and acceptors (long-range electron transfer).[38−43] Accordingly, there is a continued interest in polyprolines, which is augmented by the biological importance of proline-rich sequences.[61,62] One particularly interesting aspect is the length of the polyproline backbone, in particular when it

(56) van Gunsteren, W. F.; Billeter, S. R.; Eising, A. A.; Hünenberger, P. H.; Krüger, P.; Mark, A. E.; Scott, W. R. P.; Tironi, I. G. *Biomolecular simulation: The GROMOS96 manual and user guide*; vdf Hochschulverlag: ETH Zürich, Switzerland 1996.
(57) Wu, W.-J.; Raleigh, D. P. *Biopolymers* **1998**, *45*, 381−394.
(58) Haas, E.; Wilchek, M.; Katchalski-Katzir, E.; Steinberg, I. Z. *Proc. Natl. Acad. Sci. U.S.A.* **1975**, *72*, 1807−1811.
(59) Haas, E.; Katchalski-Katzir, E.; Steinberg, I. Z. *Biopolymers* **1978**, *17*, 11−31.
(60) Englert, A.; Leclerc, M. *Proc. Natl. Acad. Sci. U.S.A.* **1978**, *75*, 1050−1051.

adopts the PPII helix structure. There is a broad agreement that for $n = 12$ the D−A distance in polyprolines amounts to 40 ± 5 Å (Table 1).[2,15−17] Accordingly, one expects a D−A distance of ca. 20 ± 2.5 Å for $n = 6$ by additivity, or less, if one recalls that the extended PPII structure is destabilized in certain short polyprolines.[28,29] Nevertheless, single molecule fluorescence measurements, which employed FRET pairs of the Alexa dye type, returned unrealistically large apparent distances between 33 and 41 Å for $n = 6$ (Table 1).[15−17] Two likely explanations are (*i*) the large R_0 values (51−54 Å) of the employed FRET pairs, since distance determinations are generally thought to be most accurate within 0.5 R_0 to 2 R_0,[8] and (*ii*) the breakdown of the point-dipole approximation[63−67] (in Förster theory) for the large Alexa dyes. The original FRET pair selected by S&H for $n = 1−12$ (Naph/Dns)[2] and that tested by Lakowicz et al. (Trp/Dns)[19] for $n = 6$ do offer some advantages for the investigation of short polyprolines and already afford reasonable distances for $n = 6$ when calculated according to eq 1 (20 and 23.4 Å, Table 1). However, their R_0 values are still too large (27.2 and 24.2 Å) to allow the investigation of even shorter polyprolines, and both sets of previous measurements were restricted to organic solvents.[2,19]

A Spectroscopic Ruler for Short Polyprolines. The experimental investigation of D−A distances in short polyprolines required therefore the choice of an FRET pair with largely different qualities. We selected the Trp/Dbo FRET pair due to its short R_0 value of ca. 9 Å (Table 2). Moreover, the sizes of the chromophores, and in particular of the acceptor, are very small (ca. 5 Å), such that the point-dipole approximation[63,64,67] should still be valid at the investigated short distances. Finally, also problems related to orientational averaging (*cf.* Supporting Information) during the excited-state donor lifetime should be less critical, especially in water, owing to the faster rotational motions of the very small and flexibly attached chromophores as well as the longer intrinsic donor lifetime (ca. 2 ns for Trp-$(Pro)_4$-NH_2 *versus* 0.27−0.45 ns for the Alexa dyes).[16,17] The Trp/Dbo FRET pair has the additional advantage of a selective donor excitation and high water solubility of the acceptor, which allows measurements of labeled peptides in water.[18,22]

We selected peptides with the structure Trp-$(Pro)_n$-Dbo-NH_2 ($n = 1$, 2, 4, and 6, Scheme 1) for our investigations. Two design criteria were applied to ensure an early nucleation of the PPII structure in these short peptides and thereby facilitate distance interpretations and comparisons with longer polyprolines: (1) The Trp acceptor was positioned at the amino terminus because carboxy-terminal aromatic amino acids are known to disrupt the PPII helix of short polyprolines.[29,51] (2) The carboxy terminus was amidated because a deprotonated carboxy terminus is also known to disfavor the PPII helix.[28,36,37] Indeed, CD spectra (see Results) confirmed the desired early nucleation of a PPII helical structure for $n \geq 2$.[45] Accordingly, we interpret the D−A distances obtained from the FRET data in terms of separations within a PPII helix (and the linkers and tethers of the chromophores).

The Trp/Dbo pair afforded FRET efficiencies in the range 2−72% for $n = 1−6$ (Table 4), which were ideally suited for the short polyprolines of interest. Simple estimates based on the increment value of 3.12 Å per $C_\alpha−C_\alpha$ spacing in a *trans* proline bond[3] suggest separations of 3.12, 6.24, 12.48, and 18.72 Å for $n = 1$, 2, 4, and 6. Already a quick inspection reveals a surprising performance of the Trp/Dbo FRET pair, certainly for water as solvent: the transfer efficiencies for $n = 1$ and 2 are larger than 50%, because their D−A distances are shorter than the R_0 value (ca. 9 Å), while those for $n = 4$ and 6 are smaller than 50%, because their D−A distances are larger than R_0. In contrast, the FRET efficiencies of the previously employed D/A pairs fell into the less diagnostic range 74−100% for $n \leq 6$ (Table 1). Such high FRET efficiencies are generally difficult to quantify and analyze accurately, among others, due to the well-recognized problem of incomplete postcolumn *acceptor* labeling;[8,16] the latter results, if not corrected for, in apparent efficiencies which are too low and extracted distances which are too large, with the absolute error being largest for large FRET efficiencies.

The effective D−A distances recovered from eq 1 (steady-state fluorescence), eq 2 (time-resolved fluorescence), and the contour lengths recovered by distribution function analysis according to eq 3 both with a wormlike-chain model (Table 5) and a Gaussian model function (Table S-2 in Supporting Information) all provided comparable results, as expected for narrow distributions. Strikingly, the recovered D−A distances from the Trp/Dbo FRET pair for $n = 6$ (ca. 16 Å) fell significantly below those obtained for FRET pairs with 2.5 to 6 times larger R_0 values (20−41 Å, Table 1). The values obtained for the Trp/Dbo-labeled $n = 6$ hexaproline compare, however, well with (*i*) the value projected from the longer $n = 12$ dodecaproline (20 ± 2.5 Å, see above), (*ii*) independent NMR measurements in D_2O (18.6 Å),[68] (*iii*) our results from MD calculations (ca. 18 Å, Table 6), and (*iv*) the *a priori* expectation derived from the increment for *trans* proline residues[3] (18.72 Å). The trend toward slightly shorter distances afforded by the Trp/Dbo pair is presumably due to the extra two amino acids through which donor and acceptor are (flexibly) attached, e.g., the chromophores presumably fold back along the helix rather than adopt extended conformations (*cf.* MD simulations). An alternative explanation for the observed trend toward shorter calculated distances for the longer peptides could be related to the residual occurrence of *cis* Pro−Pro peptide bond conformations.[17]

The effective distances afforded for the shortest peptides increase from 7.8 to 12.3 Å in water for $n = 1−4$ (Table 5), while the MD simulations afforded 7.3−11.3 Å (Table 6, D−A distances for *trans* conformer). Unfortunately, a direct comparison of these short distances with the only literature set of data (in ethanol)[2] is not possible: The peptides studied by S&H did not adopt a PPII helical conformation at $n < 5$, while the presently investigated peptides were designed such that the PPII helix nucleates already at very short peptide length ($n \geq 2$). Moreover, the short S&H peptides suffer from nearly quantitative FRET (95−100%, Table 1), such that the extracted distances are subject to a larger error. Nevertheless, the effective distance we obtained for $n = 4$ (12.3 Å in water) compares favorably

(61) Williamson, M. P. *Biochem. J.* **1994**, *297*, 249−260.
(62) Kay, B. K.; Williamson, M. P.; Sudol, M. *FASEB J.* **2000**, *14*, 231−241.
(63) Wong, K. F.; Bagchi, B.; Rossky, P. J. *J. Phys. Chem. A* **2004**, *108*, 5752−5763.
(64) Singh, H.; Bagchi, B. *Curr. Sci.* **2005**, *89*, 1710−1719.
(65) Saini, S.; Singh, H.; Bagchi, B. *J. Chem. Sci.* **2006**, *118*, 23−35.
(66) Scholes, G. D. *Ann. Rev. Phys. Chem.* **2003**, *54*, 57−87.
(67) Wiesenhofer, H.; Beljonne, D.; Scholes, G. D.; Hennebicq, E.; Brédas, J.-L.; Zojer, E. *Adv. Funct. Mater.* **2005**, *15*, 155−160.
(68) Jacob, J.; Baker, B.; Bryant, R. G.; Cafiso, D. S. *Biophys. J.* **1999**, *77*, 1086−1092.

with the increment value expected for a PPII helix (12.5 Å). Those for $n = 1$ and 2 (ca. 8 Å) are larger than the simple increment values (3−6.5 Å), because the amino acids through which the chromophores are attached add to the actual separation; compare the MD-calculated structures in Figure 6. Consequently, the attachment mode appears to exhibit two distinct effects: it increases the separation for the shortest peptides ($n = 1$ and 2) but decreases it slightly for the longer peptides due to the "back folding" along the helical backbone ($n = 6$). These two effects balance each other for $n = 4$, where the agreement between the effective D−A distance and the proline increment value is best. This crossover is also observed in the MD simulations, where the D−A distance for the shortest peptide ($n = 1$) is longer than the calculated $C_\alpha - C_\alpha$ distance, while that for the longest peptide ($n = 6$) is shorter (Table 6). As can be seen from the foregoing, for the short polyprolines under consideration here, knowledge of the actual structures and modes of attachment of the chromophores is particularly important to understand relative and absolute variations.

Solvent Effects. The effective D−A distances indicate similar or slightly larger separations in propylene glycol compared to water as solvent, and the same trend applies for the contour lengths extracted by fitting the time-resolved FRET data according to a wormlike chain distribution function (Table 5). The latter fitting yields also the persistence lengths as a measure of the chain flexibility. It should be mentioned here that the fitting with distance distributions is model-based, and the error is large. The latter is particularly true for the persistence lengths, which were found to be significantly larger in propylene glycol (220 ± 40 Å) than in water (30−70 Å); *cf.* Table 5. The combined data suggest that the PPII helix is stabilized and that the peptides become consequently more elongated and rigid in propylene glycol compared to water. Although the underlying reasons for this trend are unknown, it is consistent with the observation of Mattice and Mandelkern, who observed that polyprolines adopt a less extended PPII structure in water than in organic solvents.[69] Alternatively, the trend toward longer contour lengths in propylene glycol could be related to our approximations in the calculation of the Förster radii, in particular, the assumption of orientational averaging ($\kappa^2 = {}^2/_3$) and of the absence of diffusion-enhanced FRET (*cf.* Supporting Information).

The absolute persistence lengths are of interest as well. The values in propylene glycol (220 ± 40 Å for $n \geq 2$) closely resemble early estimates derived from simple polymer models by assuming a fixed backbone dihedral angle ϕ.[50] Persistence lengths on the order of 220 Å should allow a reasonable modeling of polyprolines (including longer ones with $n = 12-40$) as rigid rods,[17] and our experimental data suggest that this treatment may be applicable in propylene glycol. In contrast, the persistence lengths in water fell significantly below this value even for the "longer" peptides investigated in our study ($n = 2-6$), for which we obtained a value of 30−70 Å. This indicates that these peptides have a sizable flexibility but are expectedly much less flexible than the Gly-Ser repeat peptides previously investigated by the same FRET method (l_p ca. 10 Å).[18] The persistence lengths extracted for the short PPII helices ($n = 2-6$) in water are in excellent agreement with those recently derived for longer PPII helices ($n > 12$) from single molecule fluorescence experiments, both by Schuler et al. (44 ± 9 Å)[15] and by Yang and co-workers (ca. 23 Å);[17] the latter value is also the one derived from osmometric experiments in water.[69] The present data reveal that the onset of the semirigidity occurs *in water* already for very short polyprolines. The shortest polyproline ($n = 1$) presents an exception, because its apparent persistence length is significantly larger in water (130 Å). This appears to be a general observation for very short peptides, e.g., it was also observed for the shortest Gly-Ser peptide[18] and is presumably a reflection of the limited conformational space of such short peptides, as well as the inadequacy of applying a chain-type (bio)polymer model to such short structures.

Table 7. Donor−Acceptor Distances in Rigid Structured (proline) *versus* Flexible Random-Coiled (glycine-serine) Peptides of the Type Trp-X-Dbo-NH_2 in Propylene Glycol

	R_{eff}/Å by FRET		R_{eff}(D–A)/Å by MD simulations	
n [m]	X = $(Pro)_n$[a]	X = $(Gly\text{-}Ser)_m$[b]	X = $(Pro)_n$ (*trans*)[c]	X = $(Gly\text{-}Ser)_m$[b]
2 [1]	10.3	9.1	8.9	8.0
4 [2]	13.1	9.9	11.3	8.2
6 [3]	16.5	10.4[d]	18.0	9.0[e]

[a] From Table 5. [b] From Table S-2 of ref 18. [c] From Table 6, values for *trans* isomer. [d] Unpublished results, $E_{ss} = 0.37$. [e] Unpublished results.

Comparison with Flexible Peptides. Instructive is also the comparison of the distances obtained for the rigid Trp-$(Pro)_n$-Dbo-NH_2 and the highly flexible Trp-$(Gly\text{-}Ser)_m$-Dbo-NH_2 peptides investigated in our preliminary study.[18] Table 7 compares distances obtained with the same Trp/Dbo donor/acceptor pair for peptides with the same number of amino acids in propylene glycol (diffusion-enhanced FRET contributes in the case of the flexible peptides in water as solvent). The D−A distances are consistently larger for the polyprolines, and the deviation becomes more pronounced as the length of the peptide increases from 2 to 6 amino acids. This trend reflects the higher propensity of the polyproline backbone to adopt an extended conformation in the form of the PPII helix, while the Gly-Ser repeat peptides are random-coiled. The difference in distance between the rigid and flexible peptides is even more pronounced when the results from MD simulations are compared (Table 7).

Limitations of FRET as Spectroscopic Ruler. The detailed inspection of the D−A distances by FRET in the hexaproline peptides, $n = 6$, reveals an alarming positive correlation between the extracted distance R and the Förster radius R_0 of the employed FRET pairs (Figure 7). It transpires that the measured distance, as assessed by eq 1, is not constant but depends strongly, with an absolute variation from 16 to 40 Å, on the FRET pair, rendering this method definitely not a universal spectroscopic ruler. The limitations of FRET appear to be particularly critical for short distances, where the influence of the linkers becomes important and where the point-dipole approximation may no longer hold for *large* chromophores, which are commonly also those with large R_0 values. For larger distances, above 30 Å, different FRET pairs yield good agreement, e.g., for the dodecaproline (Table 1). As stated above, it is commonly presumed that distances by FRET can be determined within a range of 0.5 R_0 to 2 R_0. The present results suggest that the lower limit, in particular, should be set more conservatively at 0.7−0.8 R_0; i.e., distances much shorter than

(69) Mattice, W. L.; Mandelkern, L. *J. Am. Chem. Soc.* **1971**, *93*, 1769−1777.

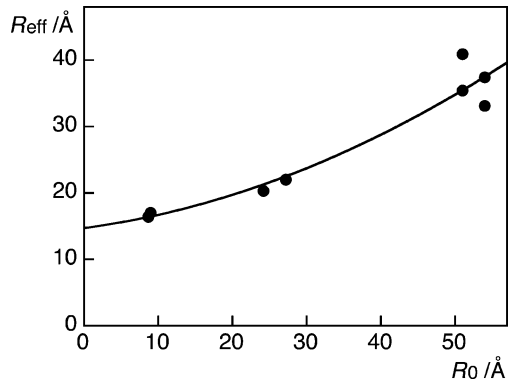

Figure 7. Dependence of the effective end-to-end distances of donor−acceptor-labeled hexaproline peptides ($n = 6$) derived from experimental FRET efficiencies according to eq 1 in dependence on the R_0 value of the employed FRET pair (data taken from Table 1). The line was obtained by fitting with a second-order polynomial function and is solely included to underscore the trend.

R_0 are less reliably assessed by FRET. Accordingly, the determinations of short distances require FRET pairs with very short Förster radii, such as the Trp/Dbo pair examined herein, to allow reasonable absolute distances to be extracted. Important to emphasize, such short-distance measurements are presently restricted to ensemble measurements, because the donors (and acceptors) of reported FRET pairs with low R_0 values[18,70−72] are unsuitable for single molecule fluorescence detection as a consequence of the required UV excitation and their low absorption cross sections.

Conclusions

In summary, an FRET pair with a very short Förster radius as the Trp/Dbo pair employed herein is essential to assess D−A separations in short polyprolines ($n \leq 6$). FRET pairs with very large R_0 values, such as those popular for single molecule detection, are preferable for longer polyprolines ($n \geq 12$) but afford too large distances for short polyprolines. For the longer polyprolines, on the other hand, the extracted distances are smaller than expected as a consequence of the sizable flexibility of polyprolines.[15,17] In view of these combined limitations for the use of FRET in both long and short polyprolines, it has been fortunate that Stryer and Haugland were able to provide early[2] on the experimental evidence for Förster theory which had then sought for, and which has contributed so much to, the application of this photophysical tool in the chemical and biological sciences.

From a methodological point of view, we have established the Trp/Dbo FRET pair as a unique and convenient tool to investigate distance relationships in very small "molecules". In particular, for donor−acceptor "dyads" separated by only 1−2 rigid amino acids, the FRET efficiencies lie in the desirable range 25−75%, which allows for accurate distance determinations in the 10-Å domain as a consequence of the steep R^{-6} dependence.[13] The resulting 10-Å spectroscopic ruler could be potentially employed to study—with high spatial resolution—supramolecular conformational changes,[73] allosteric effects,[74−76] induced-fit binding phenomena,[77] protein folding events,[78] and domain motions in proteins.[79] It is nicely complementary to NMR,[36,37,49,51,52,54,80] (electronic) CD,[2,28,29,33,38−44,46,49] and vibrational CD (VCD) spectroscopy[32,33,49] and offers additional possibilities for sensitive fluorescence detection as well as fast time-resolved measurements.

Materials and Methods

Materials. All peptides were commercially synthesized (Biosyntan, Berlin) in >99% purity ($n = 1$ and Trp-$(Pro)_6$-NH_2 reference) and >95% purity ($n = 2-6$ and $(Pro)_4$-Dbo-NH_2 reference); the FRET acceptor was introduced through the synthetic amino acid building block Fmoc-Dbo (commercially available as Puretime 325 dye from Assaymetrics, UK).[81] Propylene glycol (Fluka) was spectroscopic grade and used as received.

Spectroscopy. All measurements were performed at ambient temperature (25 °C). The fluorescence lifetimes and anisotropy decays of the peptides were measured in aerated solutions by time-correlated single-photon counting (FLS920, Edinburgh Instruments Ltd.) using a PicoQuant pulsed LED (PLS-280, $\lambda_{exc} = 280$ nm, $\lambda_{obs} = 350$ nm, fwhm ca. 450 ps) for excitation of Trp and a PicoQuant diode laser LDH-P−C 375 ($\lambda_{exc} = 373$ nm, $\lambda_{obs} = 450$ nm, fwhm ca. 50 ps) for excitation of Dbo. Rotational correlation times were determined by using an explicit correction with the g factor.[82] Corrected steady-state emission and excitation spectra and intensities ($\lambda_{exc} = 280$ nm, $\lambda_{obs} = 350$ nm) were recorded with a spectrofluorometer (Cary Eclipse, Varian). The optical density of the peptides at the excitation wavelength was spectrophotometrically (Varian Cary 4000) adjusted to ca. 0.10 for the steady-state fluorescence measurements; optically matched (±5%) solutions containing a reference peptide with known quantum yield were employed to calculate the relative fluorescence quantum yields, and residual variations in optical density at the excitation wavelength as well as variations in solvent refractive index were corrected for as described.[83]

CD spectra were recorded on a Jasco J-810 circular dichrograph (0.1 nm resolution, 10 accumulations in D_2O, 25 in propylene glycol) in 1-cm cuvettes (for D_2O) or 1-mm cuvettes (for propylene glycol). Time was taken to allow *cis-trans* Trp-Pro isomers to equilibrate (1 h in D_2O and 2 h in propylene glycol);[52,54] equilibration was verified in representative cases by measurements at different times. Peptide concentrations (ca. 20 μM in D_2O and ca. 200 μM in propylene glycol) were determined UV spectrophotometrically by assuming extinction coefficients of 5500 cm^{-1} M^{-1} and 6100 cm^{-1} M^{-1} in water[84] and propylene glycol (this work), respectively. The concentration of the reference peptide lacking Trp, i.e., $(Pro)_4$-Dbo-NH_2, was determined by using the fluorescence of Dbo upon 373-nm excitation with reference to Trp-$(Pro)_6$-Dbo-NH_2 (*cf.* Table S-3). ^{1}H NMR spectra were recorded on a JEOL JNM-ECX400 spectrometer working at 400 MHz. The pH (pD) was adjusted for the measurements in D_2O. For the measurement of the dipeptide in propylene glycol, we assumed the zwitterion (Trp-

(70) Eisinger, J.; Feuer, B.; Lamola, A. A. *Biochemistry* **1969**, *8*, 3908−3915.
(71) Wiczk, W.; Eis, P. S.; Fishman, M. N.; Johnson, M. L.; Lakowicz, J. R. *J. Fluoresc.* **1991**, *1*, 273−286.
(72) Broos, J.; Pas, H. H.; Robillard, G. T. *J. Am. Chem. Soc.* **2002**, *124*, 6812−6813.
(73) Azov, V. A.; Schlegel, A.; Diederich, F. *Angew. Chem., Int. Ed.* **2005**, *44*, 4635−4638.
(74) Arduini, A.; Giorgi, G.; Pochini, A.; Secchi, A.; Ugozzoli, F. *J. Org. Chem.* **2001**, *66*, 8302−8308.
(75) Le Gac, S.; Marrot, J.; Reinaud, O.; Jabin, I. *Angew. Chem., Int. Ed.* **2006**, *45*, 3123−3126.
(76) Ramanoudjame, G.; Du, M.; Mankiewicz, K. A.; Jayaraman, V. *Proc. Natl. Acad. Sci. U.S.A.* **2006**, *103*, 10473−10478.
(77) Lipscomb, W. N. *Proc. Natl. Acad. Sci. U.S.A.* **1973**, *70*, 3797−3801.
(78) Fersht, A. R. *Curr. Opin. Struct. Biol.* **1997**, *7*, 3−9.
(79) Hayward, S. *Proteins* **1999**, *36*, 425−435.
(80) Wüthrich, K.; Grathwohl, C. *FEBS Letters* **1974**, *43*, 337−339.
(81) Hudgins, R. R.; Huang, F.; Gramlich, G.; Nau, W. M. *J. Am. Chem. Soc.* **2002**, *124*, 556−564.
(82) Kapusta, P.; Erdmann, R.; Ortmann, U.; Wahl, M. *J. Fluoresc.* **2003**, *13*, 179−183.
(83) Mohanty, J.; Nau, W. M. *Photochem. Photobiol. Sci.* **2004**, *3*, 1026−1031.
(84) Fasman, G. D. *Handbook of biochemistry and molecular biology*, 3rd ed.; CRC: 1976.

Pro-O^-) to be dominant without additive and the protonated form (Trp-Pro-OH) to be dominant in the presence of 0.1% trifluoroacetic acid.

Molecular Dynamics Simulations. Simulations were performed with the GROMOS96 force field[56] by using the recently reported parametrization for Dbo[85] and in analogy to previous studies.[18,86] Details are contained in the Supporting Information.

Acknowledgment. Dedicated to Prof. J. Wirz, University of Basel, on the occasion of his 65th birthday. This work was supported within the graduate program "Nanomolecular Science" of Jacobs University and by the Fonds der Chemischen Industrie. The authors are grateful to Prof. B. Schuler, Prof. H. Yang, and Dr. S. Rüttinger for providing experimental raw data from refs 15−17.

Supporting Information Available: Expanded version of Table 1, details on the choice of the orientation factor, FRET efficiencies from steady-state and time-resolved fluorescence, fitting results according to Gaussian distribution function, deconvolution and analysis of acceptor fluorescence, ^{1}H NMR spectral assignments for the peptide Trp-Pro-Dbo-NH_2, discussion of diffusion-enhanced FRET, and discussion of biexponential fluorescence decays and conformations of the indole ring. This material is available free of charge *via* the Internet at http://www.acs.org.

JA072178S

(85) Roccatano, D.; Sahoo, H.; Zacharias, M.; Nau, W. M. *J. Phys. Chem. B* **2007**, *111*, 2639−2646.
(86) Roccatano, D.; Nau, W. M.; Zacharias, M. *J. Phys. Chem. B* **2004**, *108*, 18734−18742.